Title

Insights into the Dynamics and Dissociation Mechanism of a Protein Redox Complex Using Molecular Dynamics

Journal

Journal of Chemical Information and Modeling, 57(9)

ISSN

1549-9596

Authors

Hollingsworth, Scott A

Nguyen, Brian D

Chreifi, Georges

et al.

Publication Date

2017-09-25

DOI

10.1021/acs.jcim.7b00421

Peer reviewed

HHS Public Access

Author manuscript

J Chem Inf Model. Author manuscript; available in PMC 2017 November 05.

Published in final edited form as:

J Chem Inf Model. 2017 September 25; 57(9): 2344–2350. doi:10.1021/acs.jcim.7b00421.

Insights into the Dynamics and Dissociation Mechanism of a Protein Redox Complex Using Molecular Dynamics

Scott A. Hollingsworth[1,2,†], **Brian. D. Nguyen**[1,†], **Georges Chreifi**[1], **Anton. P. Arce**[1], and **Thomas. L. Poulos**[1,*]

[1]Department of Molecular Biology and Biochemistry, University of California, Irvine, CA 92697, United States

Abstract

Leishmania major peroxidase (LmP) is structurally and functionally similar to the well-studied yeast cytochrome c peroxidase (CCP). A recent Brownian dynamics study showed that *L. major* cytochrome c (LmCytc) associates with LmP by forming an initial complex with the N-terminal helix A of LmP, followed by a movement toward the electron transfer (ET) site observed in the LmP-LmCytc crystal structure. Critical to forming the active electron transfer complex is an intermolecular Arg-Asp ion pair at the center of the interface. If the dissociation reaction is effectively the reverse of the association reaction, then rupture of the Asp-Arg ion pair should be followed by movement of LmCytc back toward LmP helix A. To test this possibility we have carried out multiple molecular dynamics simulations of LmP-LmCytc complex. In 5 separate simulations LmCytc is observed to indeed move toward helix A and in two of the simulations, the Asp-Arg ion pair breaks, which frees LmCytc to fully associate with the LmP helix A secondary binding site. These results support the “bind and crawl” or “velcro” mechanism of association wherein LmCytc forms a non-specific electrostatic complex with LmP helix A followed by a “crawl” toward the ET active site where the Asp-Arg ion pair holds the LmCytc in position for rapid ET. These simulations also point to $Tyr134_{LmP}$ as being important in the association/dissociation reactions. Experimentally mutating Tyr134 to Phe was found to decrease K_m by 3.6 fold, consistent with its predicted role in complex formation by molecular dynamics simulations.

TOC image

*Corresponding author: Thomas L. Poulos, University of California, Irvine. Department of Molecular Biology & Biochemistry. Irvine, California 92697-3900 poulos@uci.edu; 949-824-7020.

[2]Current Address: Departments of Computer Science, Molecular and Cellular Physiology and Structural Biology, Stanford University, Stanford, California, 94305, United States

†These authors contributed equally to this work

Supporting Information Available

Figures S1–S5.

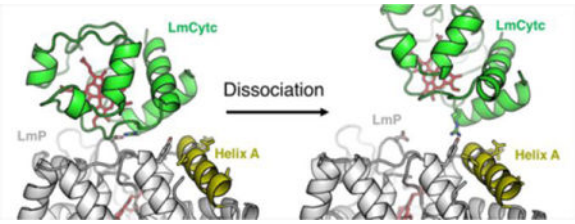

Introduction

Interprotein electron transfer requires formation of protein-protein complexes.[1, 2] Such complexes often are quite specific since the electron transfer (ET) rates between redox centers falls exponentially with distance, making it necessary to minimize the donor-acceptor distance and/or provide an appropriate ET path. Nature, however, must balance the requirement of specific binding with rapid turnover, so protein redox complexes also are designed to rapidly dissociate. Therefore, while the association rate often is quite fast, the dissociation rate also is fast which often means that neither association or dissociation is rate limiting. The resulting moderate stability of protein redox complexes is one reason why there are very few such complex crystal structures. One of the exceptions is the well-studied yeast cytochrome c peroxidase (CCP)-cytochrome c (Cytc) complex that has long served as a paradigm for interprotein ET studies.[3, 4]

Recently, a second CCP-Cytc complex has been characterized. The human pathogen *Leishmania major* has a peroxidase (LmP) that is mechanistically and structurally similar to yeast CCP.[5–8] Mechanistically, these systems have been shown to be nearly identical (Scheme 1).[6–8]

In step 1 the peroxidase is first oxidized by hydrogen peroxide to produce the ferryl compound I and a Trp radical (Fe^{IV}=O;Trp^{+}•).[9, 10] Through an electron transfer event with the related cytochrome c (step 2), the Trp^{+}• radical is reduced to give compound II (Fe^{IV}=O;Trp). An intramolecular proton-coupled electron transfer (PCET, step 3) from the Trp to Fe^{IV}=O gives Fe^{III}-OH;Trp^{+}•,[11, 12] before a second electron transfer event (step 4) with cytochrome c reduces Trp^{+}• to return the peroxidase to its resting state. In addition, the structure of the LmP-LmCytc complex is strikingly similar to the experimentally determined yeast complex.[7]

Despite their mechanistic and structural similarities, however, the LmP-LmCytc redox pair is kinetically unlike the CCP-Cytc system, which suggests that the association and dissociation of these redox pairs may be different. First, while the LmP system obeys simple Michaelis-Menten kinetics[7, 8], CCP does not.[13] Second, the crystal structure of each complex shows that the LmP-LmCytc complex is stabilized by specific intermolecular ion pairs (Fig. 1)[8] while the CCP-Cytc interface has no intermolecular ion pairs but instead appears to be stabilized by nonpolar interactions at the interface.[3] Further emphasizing the importance of electrostatic interactions in the LmP system, we recently documented a secondary binding site for LmCytc on LmP.[14] This non-catalytic site is composed of four nearly consecutive negatively charged residues on helix A, adjacent to but separate from the active site. A

combination of computational and experimental results has shown that helix A influences complex formation and dissociation for the LmP system, but not for CCP.[14] In the Brownian dynamics simulation LmCytc initially docks to LmP helix A and then migrates toward the ET active position. For the proper ET complex to form, the critically important $R24_{LmCytc}$-$D211_{LmP}$ ion pair must form at the center of the complex. The importance of this ion is underscored by the D211N mutant which exhibits ≈8% wild type activity.[14] This decrease is due to the rate limiting step switching from the Trp-to-Fe(IV)=O intramolecular ET to the rate of association of the LmCytc-LmP complex itself.[6] For the $R24_{LmCytc}$-$D211_{LmP}$ interaction to form, the intramolecular interaction between $R24_{LmCytc}$ and $E101_{LmCytc}$ must be broken, thus freeing $R24_{LmCytc}$ to adopt a new rotameric conformation in order to interact with $D211_{LmP}$.[7] These computational results guided the mutagenesis studies where removing 3 negative charges on helix A was found to lower k_{cat} by ≈3-fold and the rate of association of the two proteins by ≈6-fold.[14]

In order to study the dynamics of the LmP-LmCytc redox pair complex and provide a deeper understanding of a possible dissociation mechanism, we have carried out molecular dynamics (MD) simulations of the experimentally determined complex structure. These simulations have revealed a clear visualization of the dynamics of the important inter- and intramolecular ionic interactions, and a point of comparison to other well studied heme protein redox partner systems.

Methods

Molecular Dynamics Simulations

In order to the study the dynamics of the LmP-LmCytc complex, we conducted an initial set of three atomistic molecular dynamics (MD) simulations of the experimental co-crystal structure of LmCytc in complex with LmP (PDB ID 4GED)[7]. The preparation of the MD simulation is similar to our previous study of the LmP-LmCytc system[14] and described briefly here. Hydrogen atoms were added to the crystal structure using the psfgen plugin of VMD 1.9.1.[15] Patches were employed to connect the ferric high-spin heme with the coordinating His residues in both LmP and LmCytc while an extra bond parameter was added to describe the Met-heme coordination in LmCytc as well as the coordination of the ions present in the co-crystal structure. The surrounding orthogonal solvent box was constructed with a 20 Å cushion in all directions around the proteins. The resulting complex system contained 73,815 atoms.

The initial three MD simulations were performed using NAMD[16] version 2.10 on the greenplanet cluster at UC Irvine and the XSEDE Stampede computing cluster. The CHARMM22[17] force field was employed for the proteins and cofactor. The TIP3P model[18] was used to model the solvent. Each system underwent 1,000 steps of conjugate gradient energy minimization at a constant pressure of 1 atm and 300K using a Nosé-Hoover-Langevin piston for pressure control and a Langevin dynamics for temperature control respectively.[19, 20] A timestep of 1 femtosecond was employed for the first 10 nanoseconds of each simulation before being increased to 2 femtoseconds for the remainder of the trajectory while a multiple time step algorithm was employed to integrate the equations for motion as described previously[21]. The electrostatic interactions were treated using a smooth particle

mesh Ewald algorithm[22] and the real space part of the Ewald sum and the Lennard-Jones interactions were switched off between 10 Å and 12 Å, while the all bonds to hydrogen atoms were constrained using the SHAKE algorithm[23]. Analyses was carried out using VMD,[15],PyMOL (www.pymol.org), as well as locally developed analysis tools.

Based on the findings from the three NAMD simulations, we carried out two additional simulations using AMBER. The NAMD runs showed that once the $Arg24_{LmCytc}$-$Asp211_{LmP}$ ion pair at the LmP-Cytc interface breaks and Cytc moves toward helix A of LmP. We therefore generated the *in silico* D211A LmP mutant thus eliminating this intermolecular ion pair to see if LmCytc will undergo the same dissociation process as observed in the NAMD runs. As a control we also included a simulation with the wild type complex. The systems were prepared similarly to the NAMD runs using the same size solvent box. Ferric high-spin heme parameters were taken from Collins & Loew[24] and for the protein the AMBER ff99SB force field was used. Hydrogen mass repartitioning (HMR) through parmed was employed to redistribute the mass of the hydrogens, allowing for the use of a 4 femtosecond time step for all AMBER simulations. As part of another study, we compared simulations of cytochromes P450 with and without HMR and found little difference in the dynamics. All AMBER runs were run on the GPU clusters at the San Diego Supercomputer Center.

Site-directed mutagenesis, expression and purification

The wild type construct expressed without the N-terminal hydrophobic tail as pET28a/Δ34LmP was used for site-directed mutagenesis. The LmP Y134F mutant was prepared by PCR using the TaKaRa PrimeSTAR polymerase kit from Clontech (Mountain View, CA), and the gene was fully sequenced to ensure the fidelity of the PCR reaction. Both LmP and LmCytc were expressed and purified as previously described.[14]

Steady-State Kinetics

Spectrophotometric steady-state activity measurements were performed at room temperature on a Cary 300 UV/Visible spectrophotometer. LmCytc was reduced by adding excess sodium dithionite and incubating on ice for 30 mins. The dithionite was then removed by passing through an Econo-Pac 10DG desalting column (Bio-Rad, Irvine, CA) pre-equilibrated with 25 mM potassium phosphate, pH 6.5. All concentrations were determined using the appropriate molar extinction coefficients (ε_{558} of 29 mM^{-1} cm^{-1} for reduced LmCytc, ε_{408} of 113.6 mM^{-1} $cm^{-1}$for LmP, ε_{240} of 0.0436 mM^{-1} cm^{-1} for H_2O_2), and the rates of LmCytc oxidation were calculated using a $\Delta\varepsilon_{558}$ of 19.4 mM^{-1} cm^{-1}. All activity measurements were performed in low ionic strength 25 mM potassium phosphate pH 6.5 buffer in order to easily reach saturation of the LmCytc binding site. Activity was measured at LmCytc concentrations ranging from 5 to 40 μM. The reaction was initiated by adding 0.18 mM H_2O_2 and the oxidation of $LmCytc^{II}$ was monitored at 558 nm. All initial velocities were corrected for the enzyme-free reaction between ferrous LmCytc and H_2O_2, which accounted for about 15 % of the enzyme catalyzed rate. Data were fit according to the following hyperbolic equation:

$$\frac{V_{max} \times [LmCytc]}{K_M + [LmCytc]}$$

Results and Discussion

LmP-LmCytc Complex Dynamics

In order to study the stability of the LmP-LmCytc complex, we carried out three 650 nanosecond (ns) CHARMM MD simulations using the experimentally determined co-crystal structure[7] as a starting point. We also carried out an AMBER simulation of the wild type complex plus a second simulation where $D211_{LmP}$ has been converted to an Ala. This mutant mimics rupturing of the $R24_{LmCytc}$-$D211_{LmP}$ ion which is a critical intermolecular ion pair and the center of the complex (Fig. 1). Root mean squared deviation (RMSD) analysis (Fig. S1) showed that both LmP and LmCytc undergo large backbone deviations owing to variations in surface loops. The deviations are much less when confined to regular elements of secondary structure. This together with visual inspection of the trajectories shows that the individual structures are quite stable. However, visual inspection of the trajectories clearly showed that LmCytc moves away from the ET active site toward helix A (Fig. 2). From the crystal structure the distance between the center of mass of LmCytc and helix A is ≈26Å and shortens substantially during the simulations (Table 1) as LmCytc migrates toward LmP helix A. In CHARMM replicate 1, LmCytc first moves toward helix A, dissociates, and then re-associates with helix A. The main reason for this larger motion in replicate 1 is that the $R24_{LmCytc}$-$D211_{LmP}$ ion pair dynamically breaks and reforms throughout the simulation but remains broken after approximately 550ns which frees LmCytc to move further toward LmP helix A. The models in Fig. 2 show that toward the end of the simulations, LmCytc has moved closer to helix A in all 5 simulations. In the D211A mutant AMBER simulation, LmCytc moves to helix A much more quickly and remains there for the remainder of the simulation. The AMBER simulation of the wild type complex behaves similar to CHARMM replicate 1. The $R24_{LmCytc}$-$D211_{LmP}$ ion pair breaks at approximately 2.2 μsec and remains broken for the remainder of the simulation (Figs. 3 and S2). As in CHARMM replicate 1, breaking of the ion pair frees LmCytc to move closer toward helix A. Taken together these results show that LmCytc favors moving toward helix A but is restrained by the $R24_{LmCytc}$-$D211_{LmP}$ ion pair which prevents the full motion of LmCytc to transition from the ET active conformation to the secondary binding site of LmP helix A. Once this ion pair breaks, however, as observed in both CHARMM replicate 1 and the AMBER simulations, LmCytc is free to fully transition to the secondary binding site previously observed in Brownian dynamics simulations (helix A of LmP) and ultimately dissociates.

LmP-LmCytc Dissociation

We next focus on CHARMM replicate 1 since the $R24_{LmpCytc}$-$D211_{LmP}$ ion pair breaks relatively early and thus provides the most detailed picture of the dissociation process in the wild type complex. Once the $R24_{LmpCytc}$-$D211_{LmP}$ ion breaks and LmCytc begins to slide further toward helix A, $R24_{LmpCytc}$ forms a new interaction with $Y134_{LmP}$. As shown in Fig.

3 for both the CHARMM replicate 1 and AMBER WT simulations, the $R24_{LmpCytc}$-$Y134_{LmP}$ pair forms as soon as the $R24_{LmpCytc}$-$D211_{LmP}$ ion breaks. In the D211A AMBER simulation $R24_{LmpCytc}$ also forms an interaction with $Y134_{LmP}$. Thus in all 3 simulations where the intermolecular ion pair breaks or is not present owing to *in silico* mutagenesis, LmCytc begins its "crawl" toward helix A by initially interacting with $Y134_{LmP}$. $Y134_{LmP}$ is located between the $D211_{LmP}$ at the ET active site and the A helix (Fig. 1) and thus provides both a new H-bonding partner to $R24_{LmCytc}$ as LmCytc moves toward helix A as well as preventing reformation of the ET active ion pair with $D211_{LmP}$

The energetic incentive for LmCytc moving toward helix A during this process are two surface exposed Lys residues of LmCytc (K16 and K19) that approach E49, D50, and E54 in helix A of LmP and aid to pull LmCytc away from the ET active site. Interestingly, following breakage of this new transient interaction in CHARMM replicate 1, $R24_{LmCytc}$ again reorients and reforms an intramolecular ion pair with $E101_{LmCytc}$ that is observed in the LmCytc crystal structure in the absence of LmP (Figs. 4, 5, S3 and S4). In the wild type AMBER simulation the $R24_{LmCytc}$-$E101_{LmCytc}$ distance also decreases (Fig. S3) but not close enough to reform the iron pair. Once this change occurs, LmCytc effectively dissociates and moves away from helix A to a point where the LmCytc center of mass reaches 28 Å from its starting position in the complex crystal structure. Continuing, LmCytc then returns to LmP and where $R24_{LmCytc}$ moves back and forth between $D211_{LmP}$ and $Y134_{Lmp}$.

Kinetics of the LmP Y134F mutant

Since simulations across not only wild type and mutant complexes but also CHARMM and AMBER force fields predict that $Y134_{LmP}$ plays a role in the association/dissociation reactions, we generated the experimental $Y134F_{LmP}$ mutant and determined its kinetic parameters. Figure 6 shows a comparison of our previously determined wild type kinetics[14] with that of the $Y134F_{LmP}$ mutant. The $Y134F_{LmP}$ mutant exhibits a simple hyperbolic behavior, with a 3.6-fold increase in K_m when compared to wild type (Fig. 6), suggesting that the $Y134F_{LmP}$ mutation decreases the affinity of LmCytc for the LmP mutant. Wild type rates are restored with saturating amounts of LmCytc, as seen by the measured k_{cat} value being almost identical to wild type. This indicates that the rate-limiting step of the reaction at steady state has not changed, but remains the intramolecular proton coupled electron transfer PCET from the Trp to Fe^{IV}, as previously shown for wild type LmP[6] but that binding of LmCytc to LmP has been weakened. Together, these results suggest that the association rate constant of the LmP_{Y134F}-LmCytc complex, although impaired, remains greater than the intramolecular PCET rate constant of ~400 s^{-1}. This is consistent in the prediction of $Y134_{LmP}$ playing an important, but not vital, role in complex turnover.

Predicted Electron Transfer Rates in the LmP-LmCytc Complex

These new computational and experimental results, coupled with our previous Brownian dynamics studies,[14] indicates that helix A provides a secondary non-specific electrostatic surface to which LmCytc can rapidly bind. However, this also raises the question of whether or not LmCytc delivers electrons while hovering near helix A, or if LmCytc must move to the position observed in the crystal structure to order to transfer an electron. Since ET rates

are quite sensitive to the distance between donor and acceptor, comparing ET distances over the course of a trajectory can provide insights into which complexes are active and inactive (Figure 7 and S5). The various parameters required for this application of Marcus theory[26, 27] were taken from reference[25]: ΔG, the difference in redox potential between the $Trp208_{LmP}$ radical and $heme_{LmCytc}$, −0.5 eV and a reorganization energy of 1.0 eV[25]. In the crystal structure, the ET distance is ≈15 Å which gives a rate of $\approx 2\times10^5$ sec^{-1}. The observed rate of electron transfer from Cytc to the Trp radical using laser flash photolysis in the CCP-Cytc complex is $\approx 2\times10^6$ sec^{-1}.[25] Given the close similarity between the CCP-Cytc and LmP-LmCytc complexes, we can expect the LmP-LmCytc complex to exhibit a similar rate. It is important to note that this rate cannot be compared to the steady state rate of $\approx 460 s^{-1}$ which is the intramolecular ET from the Trp radical to Fe(IV)=O. The Cytc-to-Trp radical ET rate also cannot be compared to second order rates measured by stopped flow kinetics since stopped flow mixing experiments measure the rate of association and not intermolecular ET form the LmCytc heme to the LmP Trp radical. Therefore, any computed intermolecular ET rate well below 10^5–10^6 sec^{-1} is not compatible with the observed kinetic behavior of LmP and thus does not represent an ET active complex. In CHARMM replicates 2 and 3 (red and blue respectively), the ET rate drops 3 orders of magnitude below the experimental values of $2\times10^6 sec^{-1}$ as LmCytc moves toward helix A. In replicate 1 after LmCytc moves to helix A of LmP, the closest ET distance is ≈20 Å which gives a rate of ≈100 sec^{-1}. This is well below the both the flash photolysis rate[25] and even k_{cat}[6], which provides additional evidence that the helix A bound complex is likely inactive, as predicted by previous BD and experimental results.[14]

Conclusions

A longstanding problem in understanding biological ET reactions is the requirement for balancing specificity with a high rate of turnover. In order to maintain rapid kinetics, the formation of protein complexes must be relatively weak. On the other hand, rapid intermolecular ET requires bringing the donor and acceptor relatively close and in some cases provide the proper intervening medium for rapid ET[2]. Since the interface that must align properly for ET is small compared to the total surface area available to each protein, the probability of forming the ET active complex *via* random intermolecular collisions is small. This problem has given rise to the “bind and crawl” or “velcro”[28] model of ET, which more recently has witnessed experimental support for transient redox complexes.[29, 30] Here the redox partners initially interact *via* nonspecific complementary electrostatic surfaces. Next, the partners sample each others surface in a rapid 2-dimensional search until the more energetically favorable ET active complex is reached. However, to ensure rapid dissociation, the difference in stability between the ET active and inactive complexes must be small. The LmP-Cytc system has provided the most detailed molecular level picture on this process. Our previous Brownian dynamics work indicates that LmCytc initially forms a nonspecific complex with helix A and stays there until the $R24_{LmCytc}$-$E101_{LmCytc}$ intramolecular ion pair breaks which enables $R24_{LmCytc}$ to form an intermolecular ion pair with $D211_{LmP}$. In the present work we find that exactly the reverse happens in the dissociation reaction. The intermolecular $R24_{LmCytc}$-$D211_{LmP}$ ion pair first must break which then enables LmCytc to slide toward the helix A prior to full dissociation. In the CHARMM simulations we observe

the rupture of the $R24_{LmCytc}$-$D211_{LmP}$ ion pair in only one of the 3 simulations, but observe significant movement towards helix A in all 3 replicates. Further supporting these findings, using AMBER force fields we observe the same motions towards helix A, including breakage of the $R24_{LmCytc}$-$D211_{LmP}$ ion pair followed by formation of $R24_{LmCytc}$-$Y134_{LmP.}$ That these same specific interactions as well as the broader motions towards helix A take place across different simulation conditions increases confidence that the dynamic tug of war between the broad electronegative surface of helix A and the ET active complex controlled by the $R24_{LmCytc}$-$D211_{LmP}$ ion pair is an accurate picture on the binding/dissociation reactions. In summary, this work coupled with our previous Brownian dynamics study presents a consistent picture on the dynamics of both the association and dissociation reactions and provides further support to the “bind and crawl/velcro” model of ET protein-protein interactions and more recent advances on transient redox partner complexes.[29, 30]

Supplementary Material

Refer to Web version on PubMed Central for supplementary material.

Acknowledgments

Simulation work was supported by XSEDE grant TG-MCB130001 to SAH and the UC Irvine School of Physical Sciences Greenplanet cluster which is supported by NSF grant CHE-0840513. The authors greatly acknowledge Professors Ray Lou and Ron Dror for helpful discussions throughout this study.

This work was supported by NIH grant GM57353 to TLP, an institutional Chemical and Structural Biology Training Grant predoctoral fellowship to SAH (T32-GM10856) and an institutional Biomedical Informatics Training Grant postdoctoral fellowship to SAH (T15-LM007033-33).

Abbreviations

LmP	*Leishmania major* peroxidase
LmCytc	*Leishmania major* cytochrome c
ET	electron transfer
PCET	proton coupled electron transfer
CcP	yeast cytochrome c peroxidase

References

1. Poulos TL. Heme Enzyme Structure and Function. Chem Rev. 2014; 114:3919–62. [PubMed: 24400737]
2. Winkler JR, Gray HB. Electron Flow Through Metalloproteins. Chem Rev. 2014; 114:3369–80. [PubMed: 24279515]
3. Pelletier H, Kraut J. Crystal-Structure of a Complex Between Electron-Transfer Partners, Cytochrome-C Peroxidase and Cytochrome-C. Science. 1992; 258:1748–1755. [PubMed: 1334573]
4. Volkov AN, Nicholls P, Worrall JA. The Complex of Cytochrome c and Cytochrome c Peroxidase: the End of the Road? Biochim Biophys Acta. 2011; 1807:1482–503. [PubMed: 21820401]
5. Adak S, Datta AK. Leishmania major Encodes an Unusual Peroxidase that is a Close Homologue of Plant Ascorbate Peroxidase: a Novel Role of the Transmembrane Domain. Biochem J. 2005; 390:465–74. [PubMed: 15850459]

6. Chreifi G, Hollingsworth SA, Li H, Tripathi S, Arce AP, Magana-Garcia HI, Poulos TL. Enzymatic Mechanism of Leishmania major Peroxidase and the Critical Role of Specific Ionic Interactions. Biochemistry. 2015; 54:3328–36. [PubMed: 25941976]
7. Jasion VS, Doukov T, Pineda SH, Li H, Poulos TL. Crystal Structure of the Leishmania major Peroxidase-Cytochrome c Complex. Proc Natl Acad Sci U S A. 2012; 109:18390–4. [PubMed: 23100535]
8. Jasion VS, Poulos TL. Leishmania major peroxidase is a cytochrome c peroxidase. Biochemistry. 2012; 51:2453–60. [PubMed: 22372542]
9. Coulson AF, Yonetani T. Oxidation of cCtochrome c Peroxidase with Hydrogen Peroxide: Identification of the “Endogenous Donor”. Biochem Biophys Res Commun. 1972; 49:391–8. [PubMed: 4344886]
10. Sivaraja M, Goodin DB, Smith M, Hoffman BM. Identification by ENDOR of Trp191 as the free-radical site in cytochrome c peroxidase compound ES. Science. 1989; 245:738–40. [PubMed: 2549632]
11. Liu RQ, Miller MA, Han GW, Hahm S, Geren L, Hibdon S, Kraut J, Durham B, Millett F. Role of Methionine 230 in Intramolecular Electron Transfer Between the Oxyferryl Heme and Tryptophan 191 in Cytochrome c Peroxidase Compound II. Biochemistry. 1994; 33:8678–85. [PubMed: 8038157]
12. Miller MA. A Complete Mechanism for Steady-State Oxidation of Yeast Yytochrome c by Yeast Cytochrome c Peroxidase. Biochemistry. 1996; 35:15791–9. [PubMed: 8961942]
13. Kang CH, Brautigan DL, Osheroff N, Margoliash E. Definition of Cytochrome-C Binding Domains by Chemical Modification - Reaction of Carboxydinitrophenyl-Cytochromes-C and Trinitrophenyl-Cytochromes-C with Bakers-Yeast Cytochrome-C Peroxidase. J Biol Chem. 1978; 253:6502–6510. [PubMed: 210187]
14. Fields JB, Hollingsworth SA, Chreifi G, Heyden M, Arce AP, Magana-Garcia HI, Poulos TL, Tobias DJ. “Bind and Crawl” Association Mechanism of Leishmania major Peroxidase and Cytochrome c Revealed by Brownian and Molecular Dynamics Simulations. Biochemistry. 2015; 54:7272–82. [PubMed: 26598276]
15. Humphrey W, Dalke A, Schulten K. VMD: Visual Molecular Dynamics. J Mol Graph. 1996; 14:33–8. 27–8. [PubMed: 8744570]
16. Phillips JC, Braun R, Wang W, Gumbart J, Tajkhorshid E, Villa E, Chipot C, Skeel RD, Kale L, Schulten K. Scalable Molecular Dynamics with NAMD. J Comput Chem. 2005; 26:1781–1802. [PubMed: 16222654]
17. MacKerell AD, Bashford D, Bellott M, Dunbrack RL, Evanseck JD, Field MJ, Fischer S, Gao J, Guo H, Ha S, Joseph-McCarthy D, Kuchnir L, Kuczera K, Lau FTK, Mattos C, Michnick S, Ngo T, Nguyen DT, Prodhom B, Reiher WE, Roux B, Schlenkrich M, Smith JC, Stote R, Straub J, Watanabe M, Wiorkiewicz-Kuczera J, Yin D, Karplus M. All-atom Empirical Potential for Molecular Modeling and Dynamics Studies of Proteins. J Phys Chem B. 1998; 102:3586–3616. [PubMed: 24889800]
18. Jorgensen WL, Chandrasekhar J, Madura JD, Impey RW, Klein ML. Comparison of Simple Potential Functions for Simulating Liquid Water. J Chem Phys. 1983; 79:926–935.
19. Martyna GJ, Tobias DJ, Klein ML. Constant Pressure Molecular Dynamics Algorithms. J Chem Phys. 1994; 101:4177–4189.
20. Feller SE, Zhang YH, Pastor RW, Brooks BR. Constant-Pressure Molecular-Dynamics Simulation - the Langevin Piston Method. J Chem Phys. 1995; 103:4613–4621.
21. Grubmuller H, Heller H, Windemuth A, Schulten K. Generalized Verlet Algorithm for Efficient Molecular Dynamics Simulations with Long-Range Interactions. Mol Simulat. 1991; 6:121–142.
22. Essmann U, Perera L, Berkowitz ML, Darden T, Lee H, Pedersen LG. A Smooth Particle Mesh Ewald Method. J Chem Phys. 1995; 103:8577–8593.
23. Ryckaert JP, Ciccotti G, Berendsen HJC. Numerical integration of the Cartesian Equations of Motion of a System with Constraints: Molecular Dynamics of n-Alkanes. J Comput Phys. 1977; 23:327–341.
24. Collins JR, Loew GH. Comparison of Computational Models for Simulating Heme Proteins - a Atudy of Cytochrome c Peroxidase. Intl Nat J Quantum Chem. 1992; (S19):87–107.

25. Wang K, Mei H, Geren L, Miller MA, Saunders A, Wang X, Waldner JL, Pielak GJ, Durham B, Millett F. Design of a Ruthenium-Cytochrome c Derivative to Measure Electron Transfer to the Radical Cation and Oxyferryl Heme in Cytochrome c Peroxidase. Biochemistry. 1996; 35:15107–19. [PubMed: 8942678]
26. Marcus RA. On the Theory of Oxidation-Reduction Reactions Involving Electron Transfer. I. J Chem Phys. 1956; 24:966–989.
27. Marcus RA, Sutin N. Electron Transfers in Chemistry and Biology. Biochim Biophys Acta. 1985; 811:265–322.
28. McLendon, Control of Biological Electron Transport via Molecular Recognition and Binding: The "Velcro" Model. Structure and Bonding. 1992; 75:160–174.
29. Schilder J, Ubbink M. Formation of transient protein complexes. Curr Opin Struct Biol. 2013; 23:911–8. [PubMed: 23932200]
30. Volkov AN. Structure and Function of Transient Encounters of Redox Proteins. Acc Chem Res. 2015; 48:3036–43. [PubMed: 26606503]

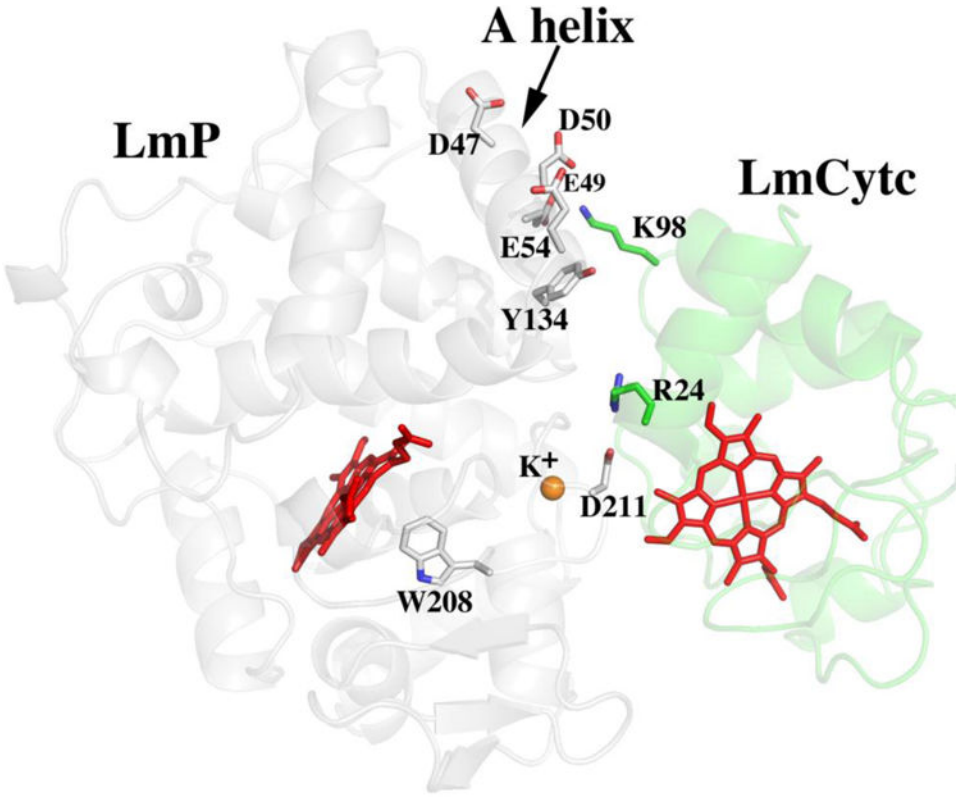

Figure 1. The LmP-LmCytc complex highlighting key interactions

LmP is in faint gray, LmCytc in faint green, and the respective heme groups are shown as red sticks. The catalytically important intermolecular ion pair between D211 of LmP and R24 of LmCytc defines the ET active binding site for LmCytc, while the negatively charged residue of D47, E49, D50 and E54 of the A helix of LmP constitutes the secondary binding site. LmP Y134 is positioned directly between the ET active and secondary binding sites.

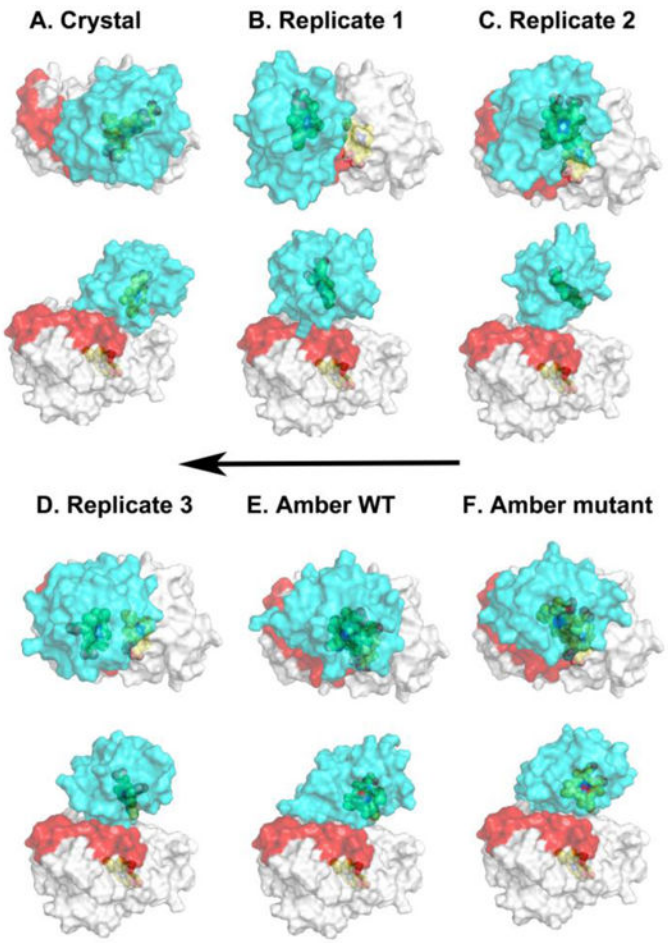

Figure 2. The LmP-LmCytc complex toward the end of simulation

Snapshots near the end of each respective MD simulation is displayed where LmCytc is cyan, LmP is white (except helix A which is shown in red). Two views are shown; one viewed down on the LmCytc docking site and a side view. A) Crystal structure; B) CHRAMM replicate 1; C) CHARMM replicate 2; D) CHARMM replicate 3; E) AMBER wild type; F) AMBER D211A mutant. Relative to the crystal structure, LmCytc moves toward the A helix in all simulations. However, in replicate 1 (panel B) and the Amber simulations (panels E and F) where the Asp-Arg intermolecular ion pair breaks, LmCytc now is free to form closer interactions with helix A. The arrow indicates the direction of motion of LmCytc.

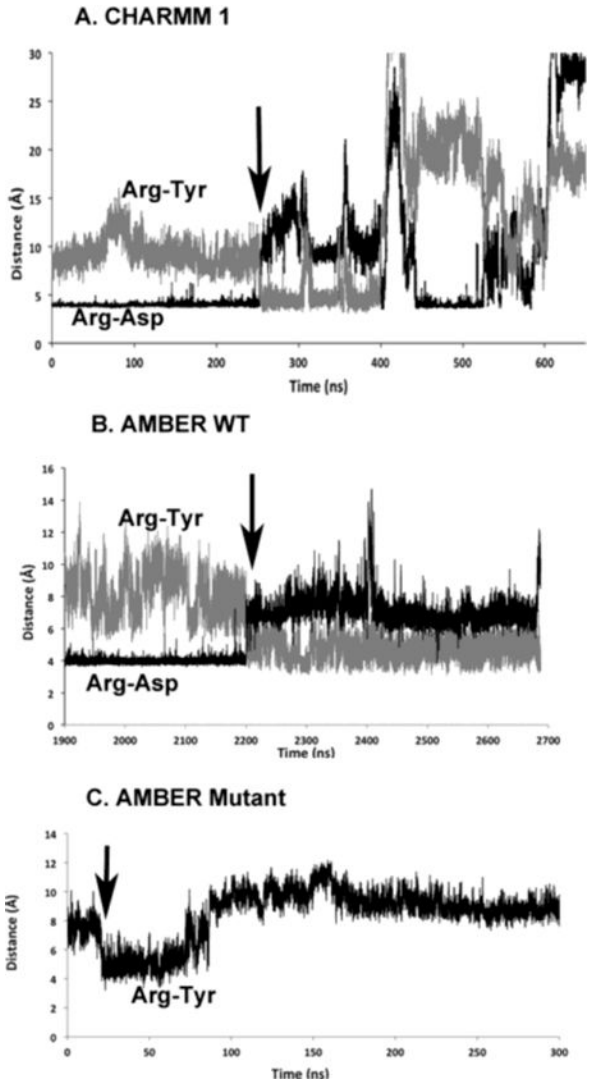

Figure 3. The $R24_{LmCytc}$-$D211_{LmP}$ and $R24_{LmCyt}$c-$Y134_{LmP}$ distances as a function of simulation time

A) CHARMM replicate 1; B) AMBER wild type; C) AMBER D211A mutant. The arrows indicate where the he $R24_{LmCytc}$-$D211_{LmP}$ breaks and the $R24_{LmCyt}$c-$Y134_{LmP}$ interaction forms. In the AMBER mutant (panel C) the $R24_{LmCyt}$c-$Y134_{LmP}$ interaction forms quickly and remains stable for about 50ns before this interaction is lost as LmCytc moves closer to helix A.

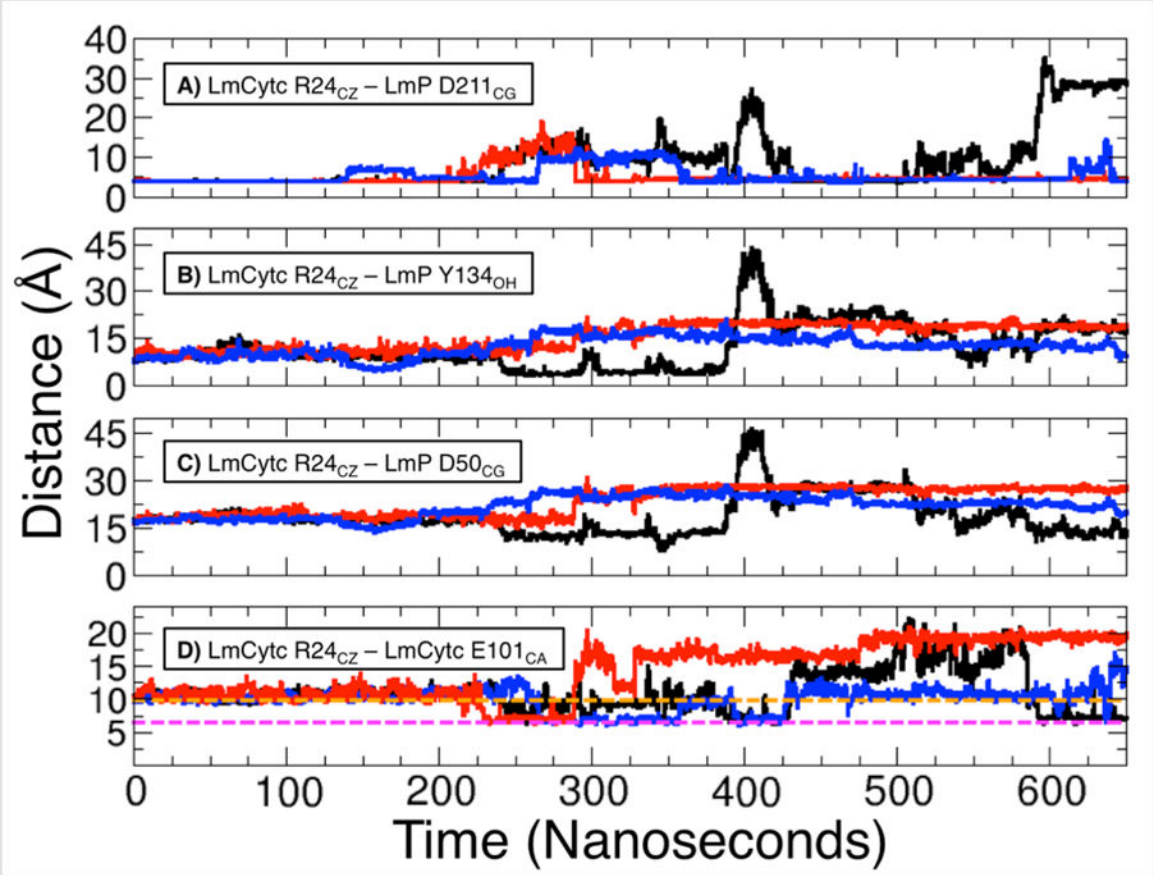

Figure 4. Distance evolution of LmP-LmCytc complex interactions

The distance between interacting residues that were found to be important during the dissociation of the LmP-LmCytc complex over the course of each 650 nanosecond MD simulation CHARMM replicates are highlighted in A through D where replicate 1 is shown in black, replicate 2 in red and replicate 3 in blue. The highlighted interactions are as follows; A) The electron transfer active interprotein ion-pair of LmCytc R24(CZ) and LmP D211(CG), B) the transient interaction between LmCytc R24(NE) and LmP Y134(OH), C) the distances between LmCytc R24(CZ) and D50 of LmP helix A and, D) the intramolecular ion pair between LmCytc R24(CZ) and LmCytc E101(CA). In D, the experimentally observed distance for the intramolecular ion pair in the individual structure (PDBID 4DY9) is shown in pink and the equivalent distance in the co-crystal structure (PDBID 4GED) in orange.

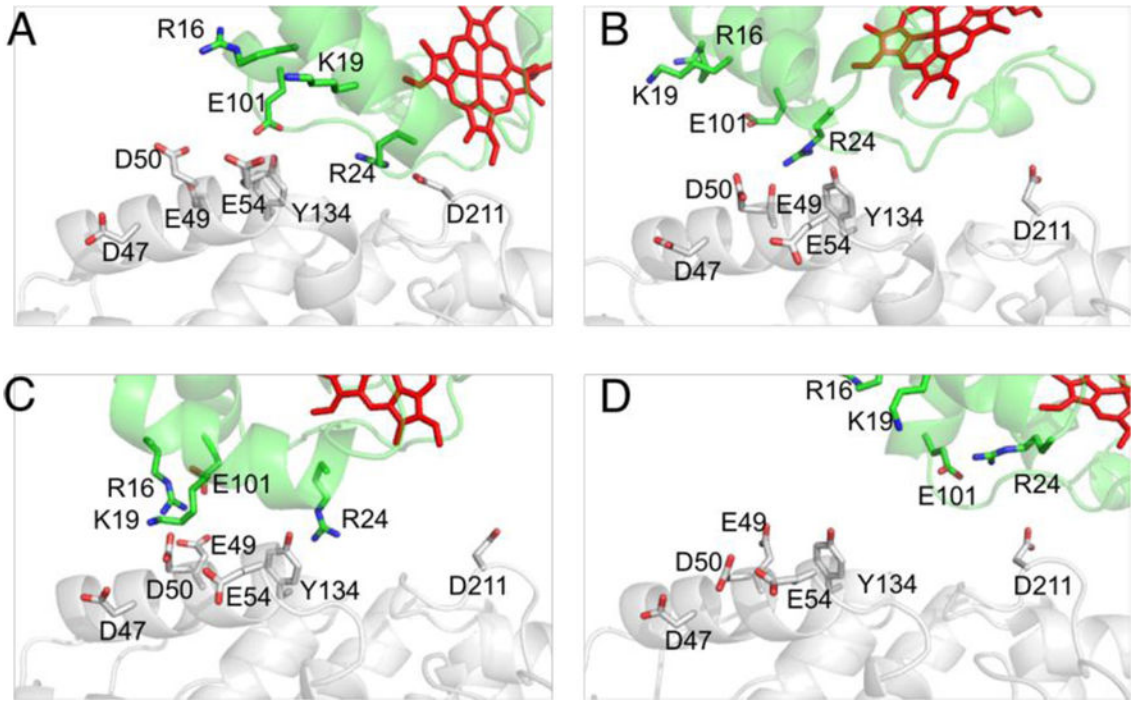

Figure 5. Snapshots of the dissociation process of the LmP-LmCytc complex

Molecular snapshots of the dissociation of the LmP-LmCytc complex as observed through the unbiased MD simulation replicate 1 taken approximately at A) 0 ns, B) 290 ns, C) 340 ns and D) 400 ns.

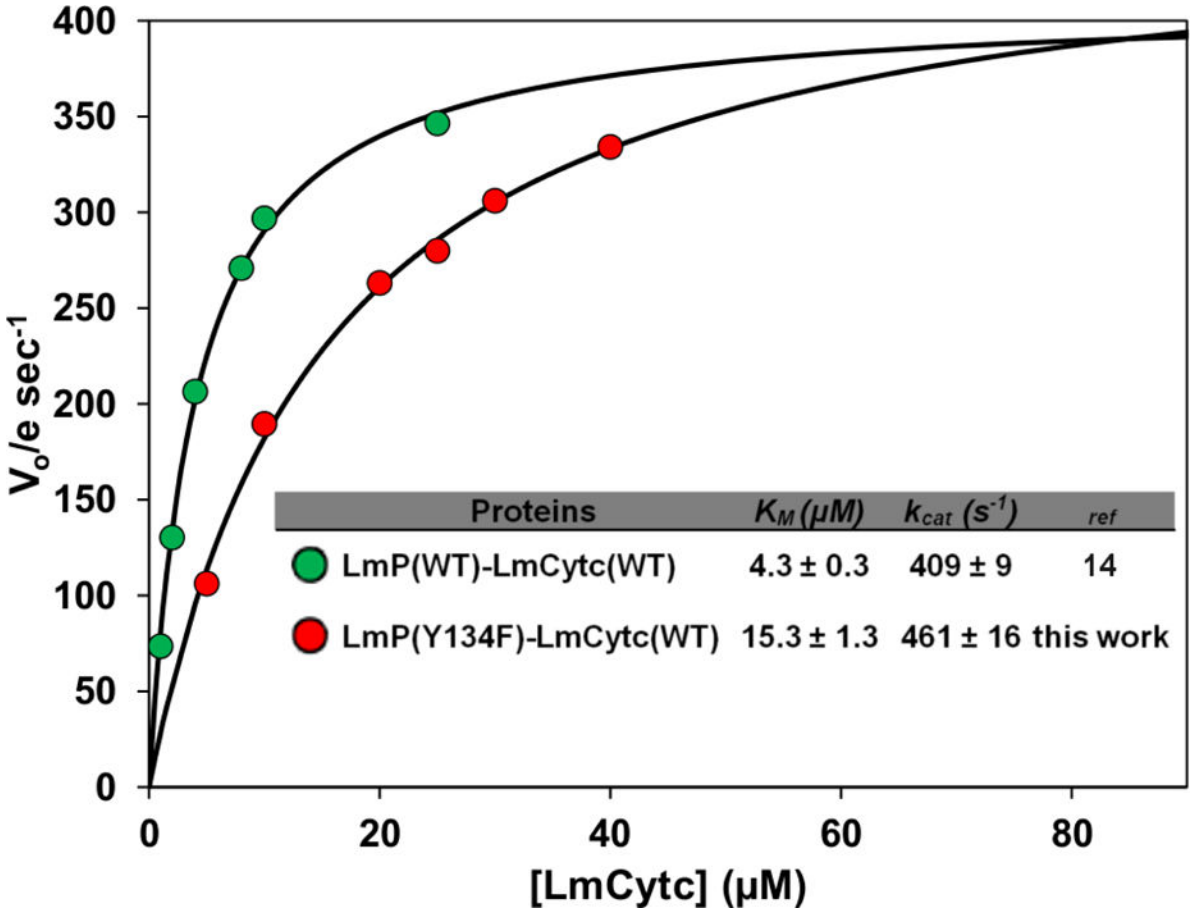

Figure 6. Experimental steady-state kinetic analysis of $Y134F_{LmP}$

V_o/e vs LmCytc concentration for the $Y134F_{LmP}$-LmCytc complex (in red) is superimposed onto the data from the wild type LmP-LmCytc complex (in green) from reference[14].

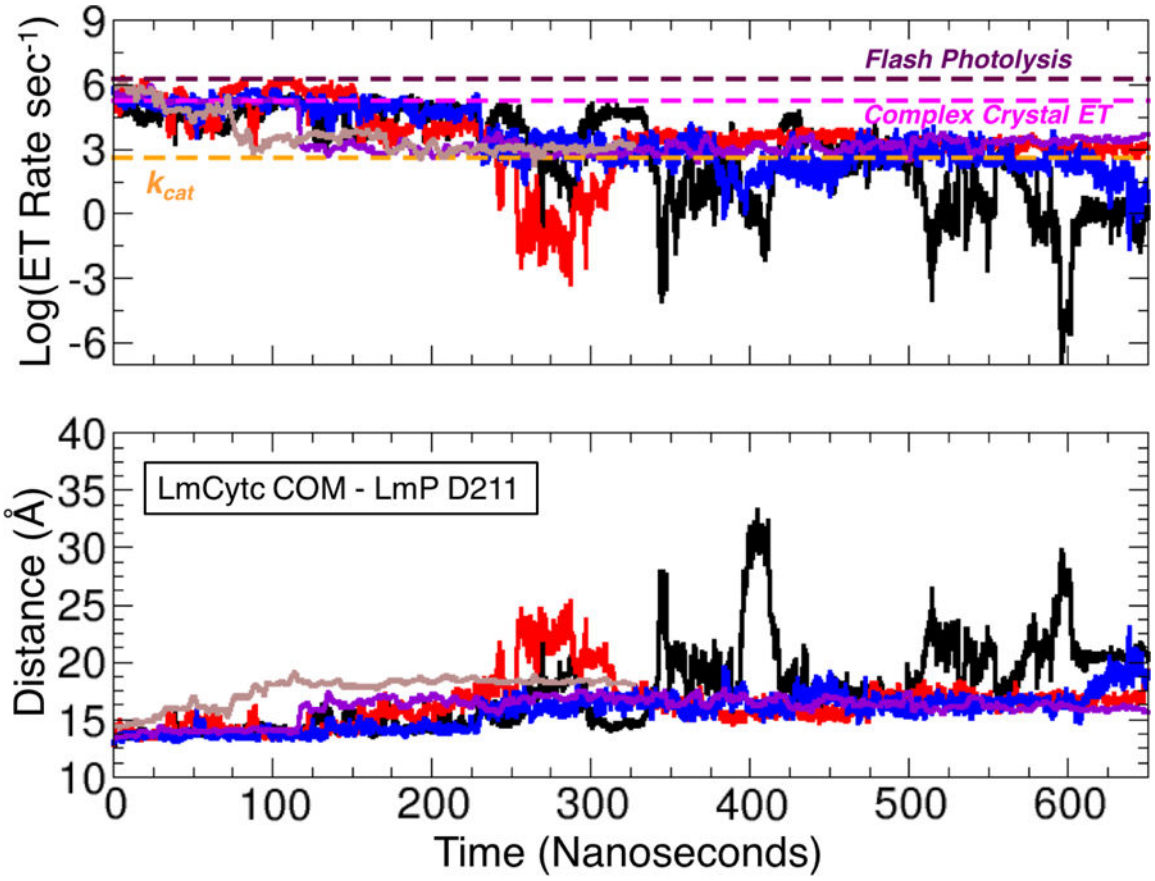

Figure 7. Predicted electron transfer distance and rate evolution for the LmP-LmCytc complex

(Top) The log of the calculated ET rate plotted as a function of time, where CHARMM replicate 1 is black, 2 is red and 3 is blue while the Amber WT simulation is purple and the mutant simulation is in light brown. The ET rate was calculated using Marcus theory as described in the text and the distance between the closest atom in the rings of $Trp208_{LmP}$ and the LmCytc heme. The dashed lines indicate the ET rate obtained from laser flash photolysis experiments for the yeast CCP-Cytc system,[25] the computed rate using the $Trp208_{LmP}$-$heme_{LmCytc}$ closest distance obtained from the LmP-Cytc structure[7], and k_{cat} obtained from steady state kinetics[6]. (Bottom) The distance between the center of mass of LmCytc and the LmP active site residue D211 over the course of each replicate is tracked using the same color scheme as above.

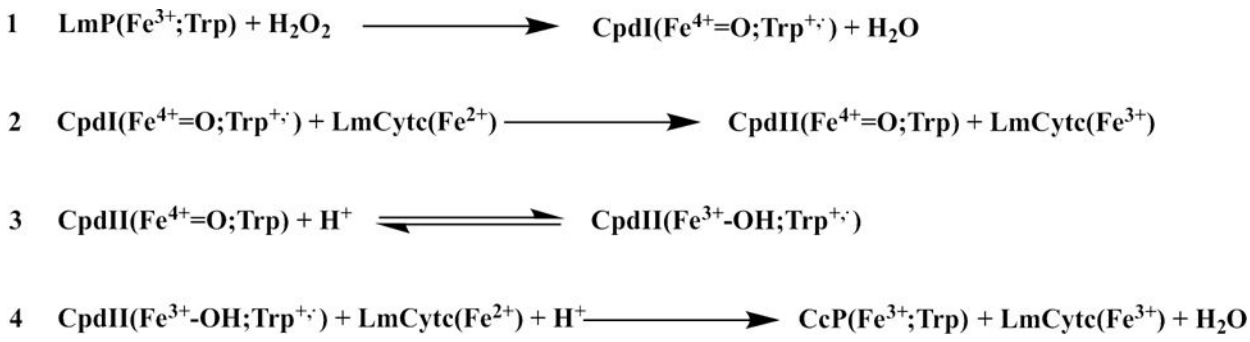

Scheme 1.
Overall Mechanism of Cytochrome c Peroxidase

Table 1

LmCytc-Helix A Minimum Center of Mass Distance

	Distance in Å
Crystal	26
CHARMM1	20.2
CHARMM2	22.4
CHARMM3	21.0
AMBER WT	20.8
AMBER Mutant	19.7